Efficient simulations at the aqueous biointerface of graphitic nanostructures with a polarisable model: Electronic Supplementary Information

Zak E. Hughes,*[a], Susana M. Tomásio[b] and Tiffany R. Walsh[a]

[a] *Institute for Frontier Materials, Deakin University, Geelong, Australia. Fax: +61 (0)3 5227 1103; Tel: +61 (0)3 5247 9160; E-mail: zhughes@deakin.edu.au*

[b] *Department of Chemistry and Centre for Scientific Computing, University of Warwick, Coventry, CV4 7AL, U.K*

Contents

Figure S10: The collective variable as a function of time for the amino acid meta-dynamics simulations for two representative systems.

Figure S11: The probability distribution of the distance between the carbon in the methyl group of Ala and the graphene surface.

Figure S12: The probability distribution of the angle between the plane of the aromatic rings and the graphene surface for the aromatic amino acid residues.

Testing of the DFT functionals

To determine the most appropriate functional for our binding energy (and distances/geometries) calculations for the full set of molecules on the graphene sheet, four different functionals were tested against a set of 13 molecules. For these 13 molecules reference data in the form of the results of DFT/CC calculations [1] and/or experimental data [2,3] was available. The adsorption energies determined for the four different functionals as well as the reference values are given in Table S2. Interestingly, the DFT/CC calculations of Rubes *et al.* found that the adsorption energies of water, ammonia and methane to graphene were equal. [1] In the case of the four functionals tested in this study, all four identified the adsorption energy of water and ammonia to be approximately equal. However, all four functionals determined the adsorption energy energy of methane as greater than water and ammonia. Indeed this failure pointed to a wider trend in that the revPBE-vdW-DF, optB88-vdW-DF and vdW-DF-C09 functionals all tended to overbind interaction of alkane molecules tested (methane, ethane and hexane) with graphene. The vdW-DF2 functional performed better regarding the adsorption energies of the alkane molecules but generally underestimated the adsorption energies of oxygen- and nitrogen-containing species. The revPBE-vdW-DF and vdW-DF2 functionals featured the lowest RMSD in terms on energies. A list of RMSD values against different sets of molecules is given in Table S3.

The separation distances between the molecules and the graphene surface are given in Table S2. The reliability of the functionals with respect to the adsorption energies is inversely proportional to their accuracy to the separation distances, with optB88-vdW-DF and vdW-DF-C09 performing better, in terms of separation distances, than revPBE-vdW-DF and vdW-DF2. This result is accordance with the findings from previous studies. [4]

Taken, together our comparison of the four different functionals indicated that the revPBE-vdW-DF functional provided the optimal balance between reliability in more adsorption energies and gave a more accurate adsorption energy for water than vdW-DF2. Thus, to determine the adsorption energies for the full set of analogue molecules the revPBE-vdW-DF functional was used. Figure S2 shows a plot of the revPBE-vdW-DF adsorption energies plotted against the reference values.

Minimum energy configurations of the aryl species

For the aryl species (benzene, toluene and phenol) the adsorption energies of the six different configurations are give in Table S4 . The prediction of the atop0 configuration (which has the centre of the benzene ring is above a carbon atom and the C-C bonds of the ring aligned along those of the graphene sheet) as the minimum energy configuration of benzene agrees with previous work [1,4]. The atop0 configuration has also been found as the minimum energy configuration of toluene on coronene, [2] however, in the present study the bri30 configuration was found to be lower in energy for toluene, however, the energy differences between the different sites were $\sim$1 kJ mol^{-1}.

Development of the GRAPPA force-field

Determination of polarisability of graphitic surfaces

The GRAPPA FF uses the rigid rod model to describe the polarisability of the graphitic surfaces. [5–7] In this model the total average dipole moment of an atom, α, is determined by

$$\alpha = \mu^2/3k_BT = q^2{l_0}^2/3k_BT \quad (1)$$

where μ is the dipole moment, q is the absolute charge on either end of the dipole and l_0 is the length of the rod. LJ interactions between graphene atoms are set to zero and the carbon atoms in the slab are held fixed in space but with the dipole on each atom free to rotate.

Langlet *et al.* a used Gaussian regularised dipole model to investigate the polarisability of carbon atoms within graphitic nano-structures. [8] Karapetian and Jordan modelled the interaction of water on graphite sheets using an out of plane polarisability of 0.86 Å^3. [9] It was found that an out of plane polarisation of 0.86 Å^3 gave good agreement with experimental data. A recent MD study of water on graphene investigated the effect of varying polarisability from 0 to 1.1 Å^3 using the Drude model to account for the polarisability of the graphene (and water molecules). [10] It was found that as the polarisability

increased so did the percentage of water molecules with one of their O-H bonds directed towards the surface.

Using the rigid rod dipole model, with a dipole on each carbon atom, with l_0 of 0.7 Å combined with a q of 0.1 e, this yielded a polarisation of 0.910 Å^3 (*c.f.* α_{Au} = 8.19 Å^3; α_{Ag} = 8.63 Å^3).[7] This gave a surface of suitable polarisability while not causing the system to become unstable or develop a significant total average dipole moment. From a 5 ns test run of a graphene sheet (one atomic layer thick) in vacuum the averaged total dipole moment per atom of a graphene sheet was $0.60 \pm 0.68 \times 10^{-4}$ D (*c.f.* Au(111) $2.8 \pm 1.4 \times 10^{-4}$ D; Ag(111) $3.0 \pm 1.4 \times 10^{-4}$ D).[7] The fictitious mass of the dipole was set to 0.5 amu.

In vacuo force-field simulation details

The adsorption energies for the GRAPPA FF were calculated using GROMACS version 4.5.5.[11] The LJ interactions were switched to zero between 9.0 and 10.0 Å while the electrostatic interactions were evaluated using the Particle Mesh Ewald (PME) method[12] with a real-space cutoff of 11.0 Å. The calculations were performed in the Canonical (*NVT*) ensemble, with the temperature maintained via the Nosé-Hoover thermostat[13,14] with a coupling constant of 0.2 ps.

A graphene surface one atomic layer thick and measuring 49.19×42.60 Å with a distance between surfaces of 60.0 Å was used to fit the force-field. The adsorption energy was calculated as the difference between the bond, angle, dihedral and vdW interactions plus half of the difference between electrostatic interactions of the adsorbed and unabsorbed systems, as detailed in previous studies.[6,15]

For the unadsorbed systems, the minimum energy configuration was determined by placing the molecule in the centre of the interslab vacuum layer and minimising the energy. For the adsorbed systems, simulated annealing MD simulations were performed. The temperature of the graphene surface was maintained at 300 K but the temperature of the molecule was reduced over 40-50 ps to 1 K as per the GolP-CHARMM method.[6] At least ten configurations were generated for each molecule.

After the minimum energy configurations had been obtained, both the adsorbed and unabsorbed configurations were simulated for 50 ps at 300 K with all particles except for the carbon dipoles fixed in position.

Fitting of force-field parameters

Using a rigid graphene sheet (one atomic layer thick) with a rigid rod dipole associated with each carbon atom with the parameters outlined above, we investigated the adsorption locations of four test molecules (water, methane, ethane and benzene). In the case of water the adsorption site, with the O atom located in the centre of a ring, was correct. By increasing the σ value of the H-C interaction it was possible to get a configuration that resembled the lowest two-leg, circumflex, revPBE-vdW-DF (and DFT/CC and AMEOBAPRO) configuration. The adsorption of the ethane and benzene molecules gave good approximations of the bridging configuration of ethane and the atop configuration of benzene. The system did not support adsorption to the correct, atop, site for methane, instead locating the adsorption site for the molecule at the centre of a ring, although the orientation of the molecule was correct (three hydrogens down). However, as ethane is a better test case for alkane species it was decided to use this set up, with the recognition that the FF is not able to capture the correct adsorption site for methane alone, while working well for alkane chains. As the energetic difference between the two found in the DFT calculations is small (0.2 kJ mol^{-1}) this is not a major defect of the FF. Ultimately it was determined that unlike in the case of the AgP/GolP-CHARMM FFs virtual sites were *not* needed to ensure the correct adsorption sites of molecules in general.

As with GolP-CHARMM/AgP-CHARMM[6,7] the parameters of the force-field were obtained through first deriving a set of C(graphene)-C(graphene) parameters, from the results of calculations of the alkane molecules with the graphene surface. After this, different species were investigated and where the generic C(graphene)-C(graphene) parameters did not capture the E_{ads}/d_{sep} of the molecule, bespoke parameters were derived. As the revPBE-DFT-dW-DF functional is known to overestimate distances,[4,6,7,16] the LJ parameters were fitted to $d_{FF} = d_{DFT} - 0.2$ Å.

It was found that using the generic C(graphene)-C(graphene) parameters with the usual CHARMM mixing rules (Lorentz-Berthelot) gave suitable E_{ads} for benzene and toluene as well as the alkanes. In the case of ethene the E_{ads} was too low and the adsorption site was also incorrect. However, as there are no unsaturated non-aromatic C-C bonds in any of the twenty natural amino-acids it was decided not to develop a set of parameters for interaction of the graphitic carbons with unsaturated aliphatic carbons at this time.

For the oxygen-containing species, hydroxyl oxygens were distinguished from amide/carbonyl oxygens. In addition, the water oxygen and hydrogen atoms required separate parameters with respect to the parameters for the other oxygen-containing molecules. The adsorption geometries obtained with the FF in general agreed with those obtained from the DFT calculations, although phenol was found to adsorbed at the atop0 rather than the atop30 position ($\Delta E_{\mathrm{ads}}^{DFT}$= 0.4 kJ mol^{-1}) and methanoic acid was found to lie at a slight angle, $\sim 17^{\circ}$, to the graphene plane rather than parallel.

For the aromatic nitrogen-containing species, imidazole and indole, no bespoke parameters wee required beyond those for polar hydrogens. Bespoke parameters were required for

methanamine and ethanamine, where the fitted parameters gave good energies and geometries but it was not possible to capture the difference in the DFT separation distances of methanamine (3.42 Å) and ethanamine (3.74 Å). The results for ammonia have been included for completeness but the final parameters were not used in the fitting process, as the amine molecules are better analogues of the lysine side chain, and N-terminus.

For sulphur it was found that one set of parameters was suitable for describing both thiol and sulphide species. As with methanamine/ethanamine, recovering the greater separation distance of the ethanethiol (3.95 Å) with respect to methanthiol (3.63 Å) was not possible.

The adsorption energies and separation distances for the full set of molecules with both the FF and the DFT calculations are given in Table S1. The root mean square deviation (RMSD) in the energies of the DFT calculations and the energies obtained using the FF was 1.66 kJ mol^{-1}for the fitting set of molecules and 1.96 kJ mol^{-1} for the validation set. By way of comparison the RMSD of the adsorption energies of the validation sets for the Au(111), Ag(111), Au(100) and Ag(100) surfaces were 4.15,[6] 3.89,[7] 3.64[6] and 2.39 kJ mol^{-1},[7] respectively.

AMEOBAPRO simulation details

The graphite surface was modelled by a three graphene sheets, each of 72 atoms, in the ABA arrangement (*i.e.* following an equivalent setup to system 3 used in the GRAPPA FF simulations). The periodic cell measured approximately $12.8 \times 14.8 \times 47.0$ Å, with 210 water molecules present in the system. The (14×0) CNT contained 67 water molecules and was 51.112 Å long (the same system set up as for GRAPPA). During the simulations the positions of the carbon atoms in both systems were held fixed.

A cutoff of 8 Å was applied for all nonbonded interactions. Long-range electrostatic interactions were evaluated using Ewald summations. A timestep of 1 fs was used for all simulations. The simulations were performed for 2 ns in the The CNT simulation was conducted in the *NVT* ensemble at 298 K, the graphene simulation was performed in the isothermal-isobaric (*NPT*) ensemble at a temperature of 298 K and a pressure of 1 atm. With the temperature and pressure maintained via the Berendsen thermostat/barostat.[17]

O-H bond vector probability distribution function

The probability distribution of the angle between the O-H bond vector and the normal of the graphene plane calculated for the water molecules in the first water layer ($r \leq 5.0$ Å) is shown in Figure S6. The results of the two FFs agree very well with each other and are in general agreement with the FPMD simulations, all giving the major peak in probability distribution at an angle of $\sim$100° with a shoulder at $\sim$20°. The FPMD studies also show a small shoulder at $\sim$160° in the tilt angle probability distribution. Using the SWM4-DP water model with a polarisable force-field for graphene Ho and Striolo showed that the probability of tilt angles of $\sim 160-180$° increased as the polarisability of the graphene sheet was increased,[10] however, the AMEOBAPRO FF is also polarisable and no shoulder was present in these data.

(14×0) CNT Simulation Timing Data

To compare the efficiency of GRAPPA against that of AMEBOBAPRO the time taken to complete 1 ns simulation, for a system of 67 water molecules within the (14×0) CNT (full simulation details described previsouly) were determined, using a single core of x86 architecture. For an additional comparison, we carried out a simulation of the same system using the standard CHARMM22* FF (*i.e.* all dipole particles were removed; all other simulation parameters were identical to the GRAPPA simulation), denoted herein as C22*. We used a single core to enable a fair, like-for-like comparison, since the the multipole-based electrostatics routines in TINKER (v6) are not parallelized.

The GRAPPA and C22* simulations took 73 and 164 minutes, respectively, compared with the $\sim$1 week needed needed for the AMOEBAPRO simulation. Thus, GRAPPA is clearly far more efficient than AMOEBAPRO while only showing a moderate increase in computational expense over the standard CHARMM22* FF.

Polarisation Contribution Tests

The contribution of the polarisability of the graphene surface to the interaction with charged species was calculated for model systems with two oppositely-charged ions (namely capped-Arg$^+$Cl$^-$ and capped-Asp$^-$Na$^+$) adsorbed onto the graphene interface, *in vacuo*. These species were considered together to ensure overall charge-neutrality of the cell. The simulation details used were the same as those used for calculation of the *in vacuo* FF energies (see the Methods section of the main manuscript, subsection '*In vacuo* force-field parameter fitting'). We performed annealing for 30ps from 300K to 1K to obtain low-energy states. The Arg$^+$/Asp$^-$ and Cl$^-$/Na$^+$ were located on the same face of the slab, but separated from each other by $\approx$ 25 Åin the *xy*-plane. Each interaction energy calculation was performed twice; once with the charge on the carbons atoms dipoles set to 0.1 *e* and once with charge set to zero. The interaction energies, and the contribution due to the polarisability, are given below:

- Arg^+/Cl^-:

  in vacuo interaction energy with charged dipoles = -172 kJ mol^{-1}

  in vacuo interaction energy with uncharged dipoles = -107 kJ mol^{-1}

  polarisation contribution = - 65 kJ mol^{-1}

- Asp^-/Na^+:

  in vacuo interaction energy with charged dipoles = -182 kJ mol^{-1}

  in vacuo interaction energy with uncharged dipoles = -77 kJ mol^{-1}

  polarisation contribution = -105 kJ mol^{-1}

Overall, it is clear that there is a significant contribution arising from the polarisability of the surface, $\sim$40 % in the case of Arg^+/Cl^- and $\sim$60 % in that of Asp^-/Na^+.

References

1 M. Rubeš, J. Kysilka, P. Nachtigall and O. Bludský, *Phys. Chem. Chem. Phys.*, 2010, **12**, 6438–6444.

2 P. Lazar, F. Karlický, P. Jurečka, M. Kocman, E. Otyepková, K. Šafářová and M. Otyepka, *J. Am. Chem. Soc.*, 2013, **135**, 6372–6377.

3 R. Zacharia, H. Ulbricht and T. Hertel, *Phys. Rev. B*, 2004, **69**, 155406.

4 K. Berland and P. Hyldgaard, *Phys. Rev. B*, 2013, **87**, 205421.

5 F. Iori, R. Di Felice, E. Molinari and S. Corni, *J. Comput. Chem.*, 2009, **30**, 1465–1476.

6 L. B. Wright, P. M. Rodger, S. Corni and T. R. Walsh, *J. Chem. Theory Comput.*, 2013, **9**, 1616–1630.

7 Z. E. Hughes, L. B. Wright and T. R. Walsh, *Langmuir*, 2013, **29**, 13217–13229.

8 R. Langlet, M. Devel and P. Lambin, *Carbon*, 2006, **44**, 2883–2895.

9 K. Karapetian and K. D. Jordan, in *Water in Confining Geometries*, ed. V. Buch and J. P. Devlin, Springer, Berlin, 2003, pp. 139–150.

10 T. A. Ho and A. Striolo, *J. Chem. Phys.*, 2013, **138**, 054117.

11 B. Hess, C. Kutzner, D. Van Der Spoel and E. Lindahl, *J. Chem. Theory Comput.*, 2008, **4**, 435–447.

12 T. Darden, D. York and L. Pedersen, *J. Chem. Phys.*, 1998, 1–6.

13 S. Nosé, *J. Chem. Phys.*, 1984, **81**, 511.

14 W. Hoover, *Phys. Rev. A*, 1985, **31**, 1695–1697.

15 F. Iori and S. Corni, *J. Comput. Chem.*, 2008, **29**, 1656–1666.

16 J. Klimeš, D. R. Bowler and A. Michaelides, *J. Phys.: Condens. Matter*, 2010, **22**, 022201.

17 H. J. C. Berendsen, J. P. M. Postma, W. F. van Gunsteren, A. Dinola and J. R. Haak, *J. Chem. Phys.*, 1984, **81**, 3684–3690.

Table S1 Adsorption energies, E_{ads}, and separation distances, d_{sep}, of the various analogue molecules and the graphene surface determined from both the DFT calculations and the GRAPPA force-field

Molecule	E_{ads} / kJ mol^{-1}			d_{sep} / Å			Set
	Ref.	DFT	GRAPPA	Ref.	DFT	GRAPPA	
Methane	-13.5[a]	-16.6	-13.3	3.31[a]	3.53	3.30	Fitting
Ethane	-20.8[a]	-23.7	-22.6	3.44[a]	3.69	3.47	Fitting
Butane		-40.5	-37.2		3.77	3.48	Validation
Hexane	-51.0[b]	-56.6	-53.6		3.78	3.51	Fitting
Benzene	-43.1[a], -48.2[c]	-46.9	-47.0	3.30[a]	3.59	3.32	Fitting
Toluene	-56.5[b]	-57.6	-55.7		3.60	3.33	Validation
Ethene	-20.2[a]	-22.6	-17.4	3.24[a]	3.52	3.35	-
Water	-13.5[a]	-13.2	-13.3	3.19[a]	3.51	3.20	Fitting
Methanol		-23.6	-24.5		3.25	3.16	Fitting
Ethanol	-30.5[b]	-29.9	-29.3		3.33	3.11	Validation
Phenol		-53.4	-53.4		3.46	3.22	Fitting
Methanamide		-28.0	-30.8		3.33	2.99	Fitting
Ethanamide		-37.2	-37.1		3.32	3.00	Validation
Methanoic Acid		-24.8	-26.9		3.38	3.14	Fitting
Acetone	-34.3[b]	-37.4	-33.1		3.28	3.03	Validation
Ammonia	-13.4[a]	-13.4	-15.7	3.31[a]	3.65	3.29	-
Methanamine		-24.3	-24.2		3.42	3.29	Fitting
Ethanamine		-31.4	-30.5		3.74	3.30	Validation
Imidazole		-39.4	-38.4		3.48	3.18	Fitting
Indole		-64.3	-64.5		3.49	3.24	Validation
Methane thiol		-27.0	-27.5		3.63	3.41	Fitting
Ethane thiol		-35.7	-36.3		3.95	3.41	Validation
Dimethyl sulfide		-35.5	-35.9		3.64	3.41	Validation
Diethyl sulfide		-52.3	-51.7		3.77	3.45	Fitting

[a] DFT/CC calculation [1]; [b] Experimental [2]; [c] Experimental [3].

Table S2 Adsorption energies, E_{ads}, and separation distances, d_{sep}, in parantheses, to graphene of the reference molecules for the various functionals

Index	Molecule	E_{ads} / kJ mol^{-1} (d_{sep} / Å)				Refence
		revPBEvdW-DF	optB88-vdw-DF	vdW-DF2	vdW-DF-C09	
1	Methane	-16.6 (3.53)	-17.0 (3.43)	-14.1 (3.43)	-17.4 (3.32)	-13.5[a] (3.31[a])
2	Ethane	-23.7 (3.69)	-25.7 (3.51)	-20.6 (3.65)	-26.6 (3.44)	-20.8[a] (3.44[a])
3	Hexane	-56.6 (3.78)	-63.2 (3.60)	-50.5 (3.71)	-64.4 (3.52)	-51.0[b]
4	Ethene	-22.6 (3.52)	-24.9 (3.29)	-19.3 (3.37)	-26.2 (3.20)	-20.2[a] (3.24[a])
5	Benzene	-46.9 (3.59)	-54.4 (3.33)	-41.4 (3.52)	-57.3 (3.24)	-43.1[a], -48.2[c] (3.30[a])
6	Toluene	-57.6 (3.60)	-66.5 (3.36)	-50.7 (3.50)	-69.2 (3.28)	-56.5[b]
7	Ethyne	-19.7 (3.49)	-21.4 (3.31)	-17.2 (3.46)	-22.1 (3.24)	-17.1[a] (3.26[a])
8	Water	-13.2 (3.51)	-13.8 (3.34)	-12.0 (3.35)	-14.1 (3.28)	-13.5[a] (3.19[a])
9	Ethanol	-29.9 (3.33)	-32.0 (3.10)	-26.3 (3.24)	-34.1 (3.03)	-30.5[b]
10	Acetone	-37.4 (3.28)	-43.1 (3.09)	-34.1 (3.18)	-45.5 (3.05)	-34.3[b]
11	Ammonia	-13.4 (3.65)	-13.5 (3.58)	-11.4 (3.52)	-14.2 (3.58)	-13.5[a] (3.31[a])
12	Acetonitrile	-29.9 (3.44)	-31.4 (3.18)	-26.2 (3.33)	-33.2 (3.17)	-31.8[b]
13	Ethyl Acetate	-51.2 (3.48)	-57.5 (3.22)	-45.6 (3.37)	-60.0 (3.16)	-48.1[b]

[a] DFT/CC calculation [1]; [b] Experimental [2]; [c] Experimental [3].

Table S3 RMSD values for adsorption energies, E_{ads}, and separation distances, d_{sep}, for the four functionals tested with different groups of molecules.

Parameter	Group of molecules (indicies)	revPBE-vdW-DF	optB88-vdw-DF	vdW-DF2	vdW-DF-C09
E_{ads} / kJ mol^{-1}	Full set with Expt. benzene value	2.61	6.35	3.10	8.11
	Full set with DFT/CC benzene value	2.82	6.96	2.38	8.48
	DFT/CC results (1,2,4,5,7,8,11)	2.54	5.41	1.24	6.68
	Expt. results (3,5,6,9,19,15,16)	2.86	8.07	4.40	10.04
$d_{sep}/Å$	DFT/CC results (1,2,4,5,7,8,11)	0.28	0.13	0.18	0.08

Table S4 Adsorption energies, E_{ads}, at different sites for the phenyl species binding to graphene (all calculations with revPBE-vdW-DF functional). The lowest energy configurations for each species are in bold text.

Site	E_{ads} / kJ mol^{-1}		
	Benzene	Toluene	Phenol
atop0	**-46.9**	-56.5	-52.9
atop30	-46.5	-57.5	**-53.4**
bri0	-46.6	-56.1	-52.1
bri30	-46.5	**-57.6**	-53.3
holl0	-45.4	-54.8	-50.9
holl30	-45.1	-56.0	-51.8

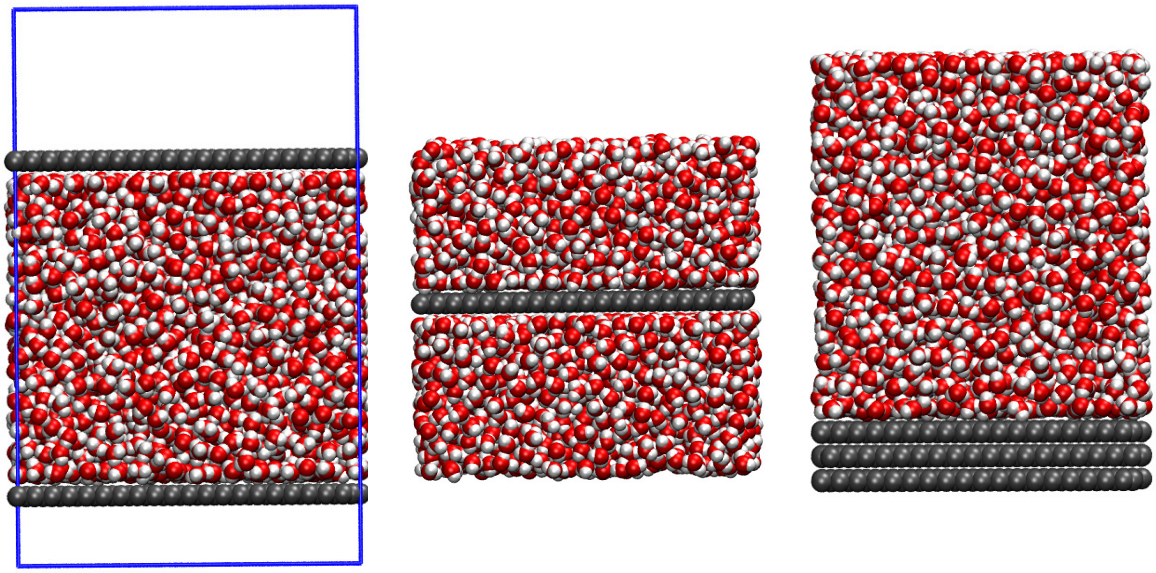

Fig. S1 System set-ups of the three different graphene-water simulations.

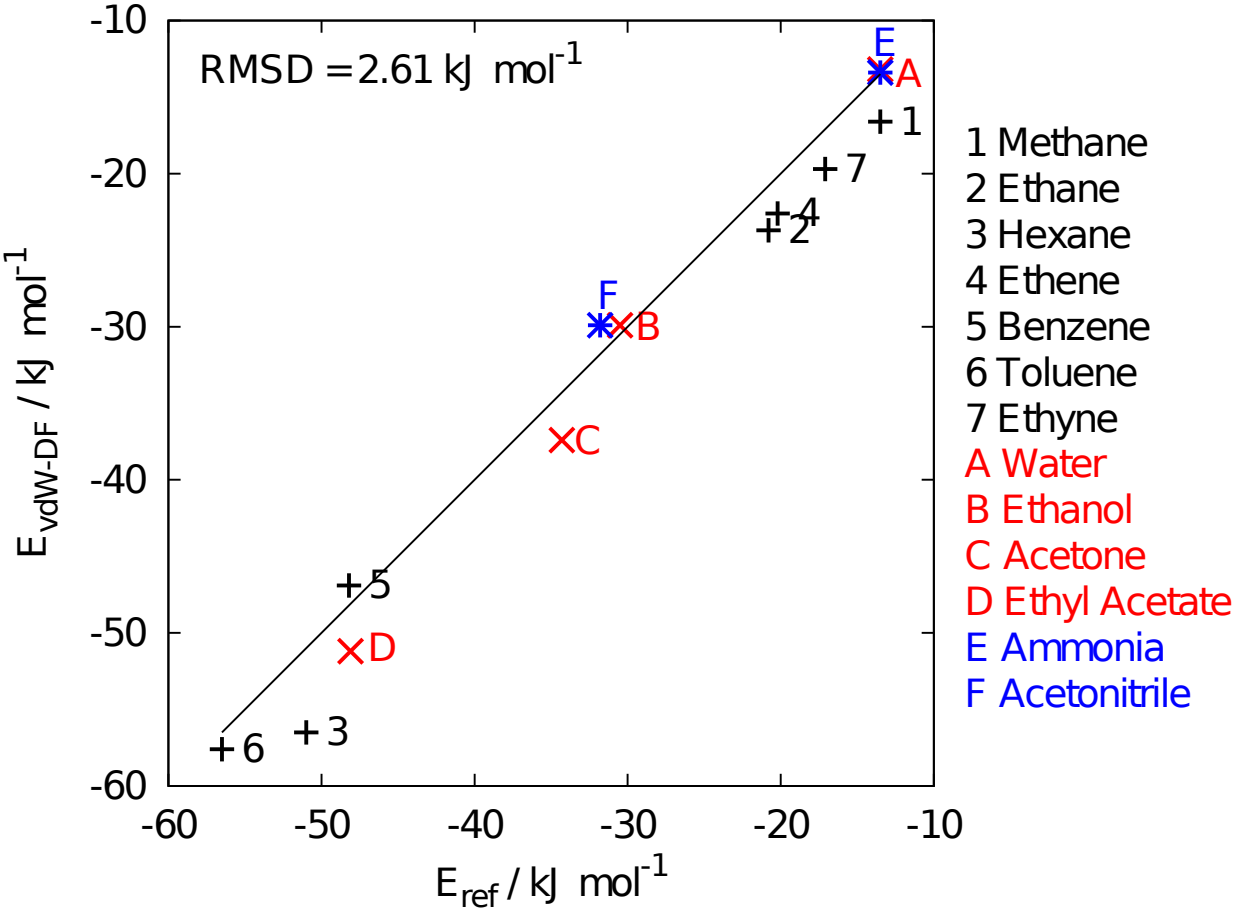

Fig. S2 Comparison between the reference adsorption energies for a set of small molecules adsorbed onto a graphene surface and those calculated with the revPBE-vdW-DF functional. The hydrocarbon, oxygen-containing and nitrogen-containing adsorbates are marked as the black, red and blue points, respectively.

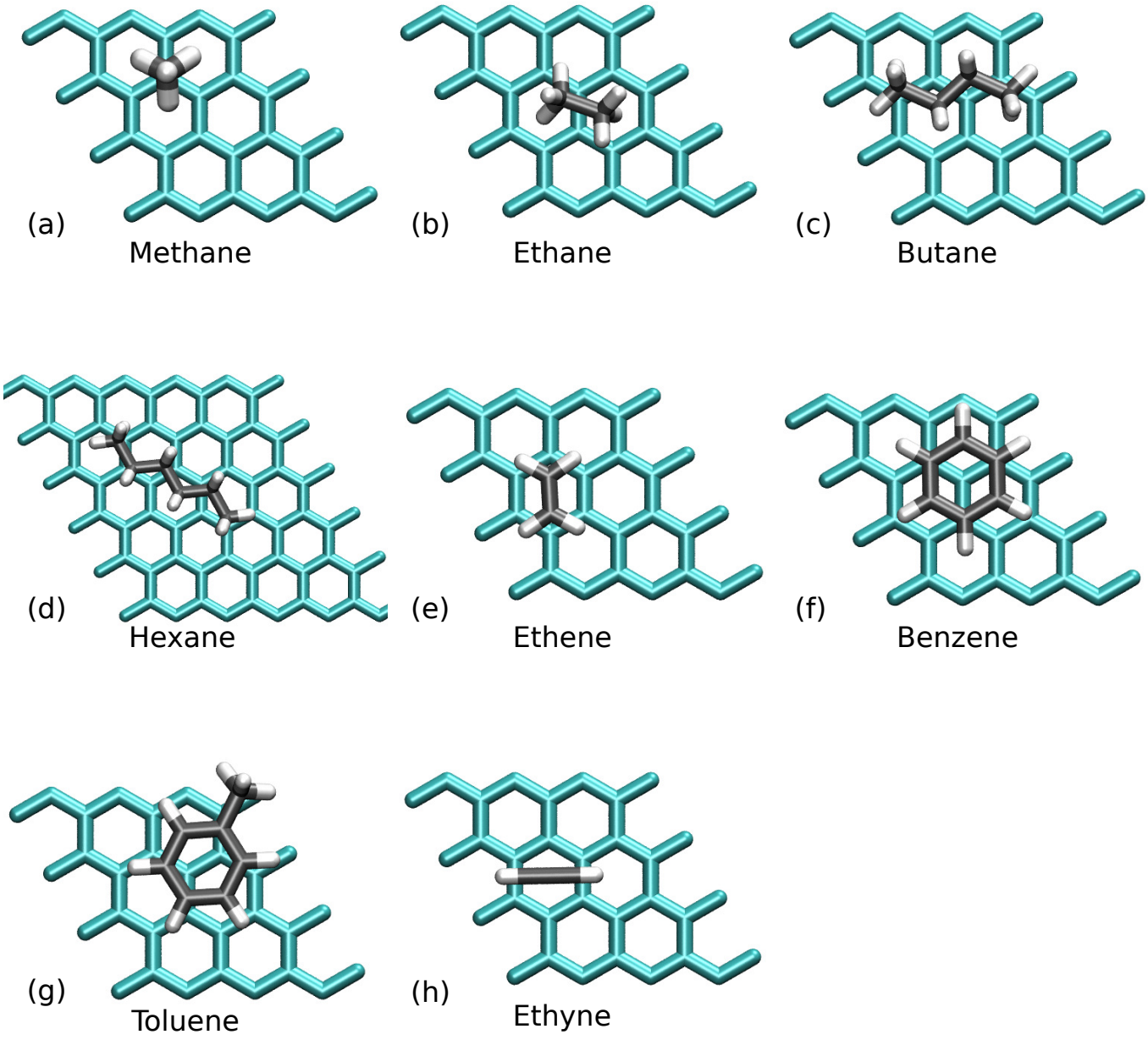

Fig. S3 The minimum energy configurations of the different hydrocarbon molecules to the graphene sheet with the revPBE-vdW-DF functional.

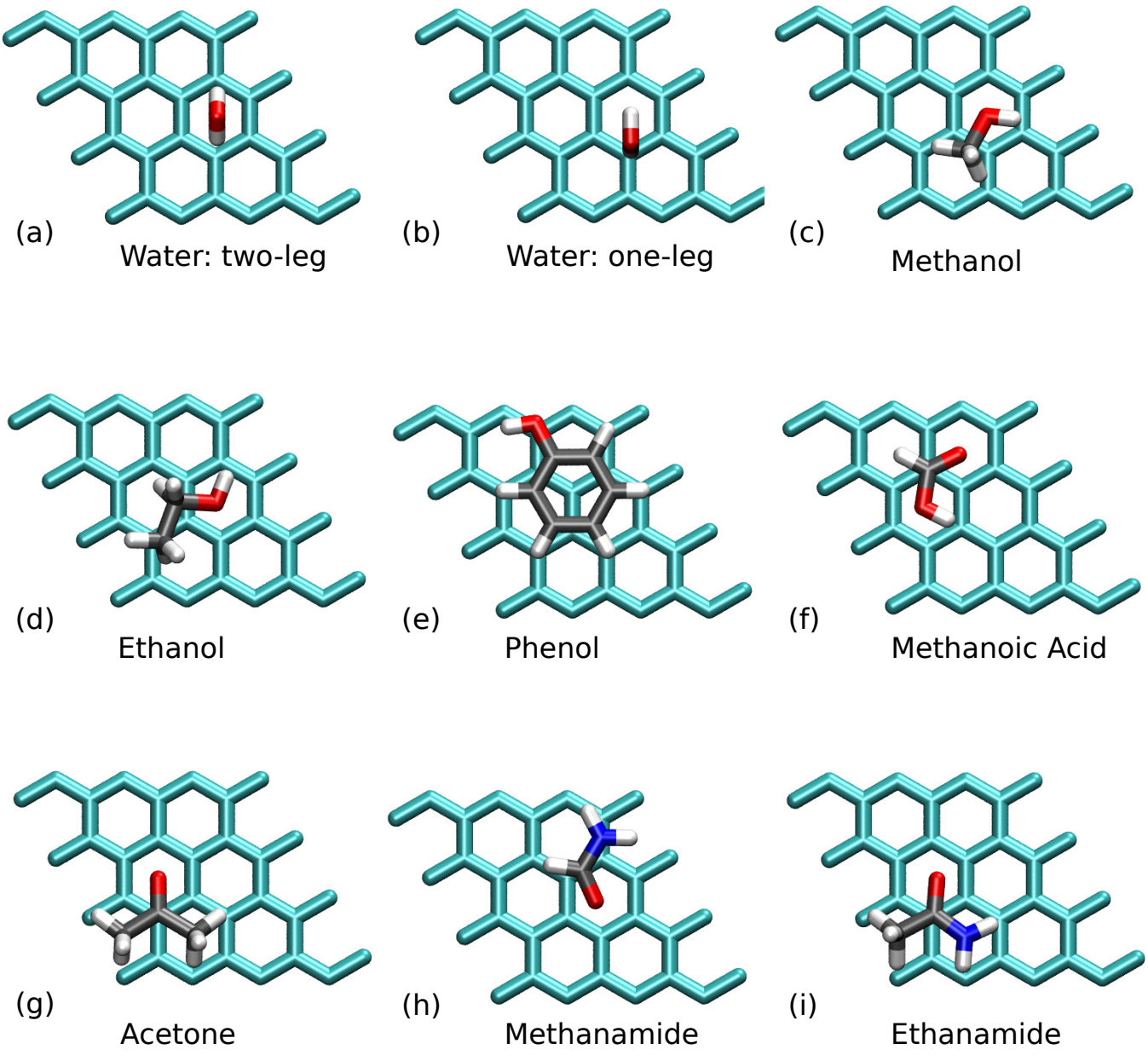

Fig. S4 The minimum energy configurations of the different oxygen containing molecules to the graphene sheet with the revPBE-vdW-DF functional.

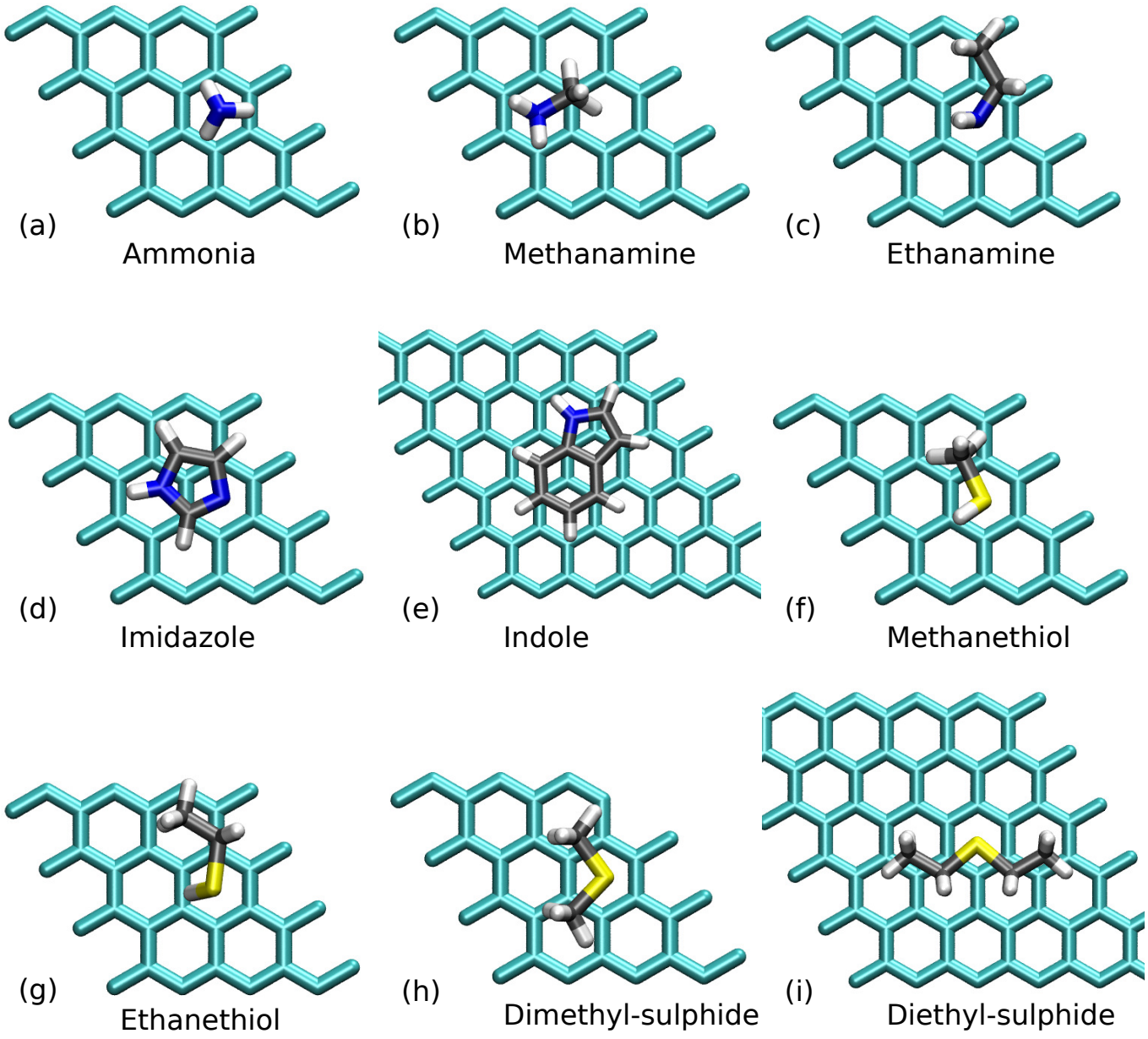

Fig. S5 The minimum energy configurations of the different nitrogen and sulphur containing molecules to the graphene sheet with the revPBE-vdW-DF functional.

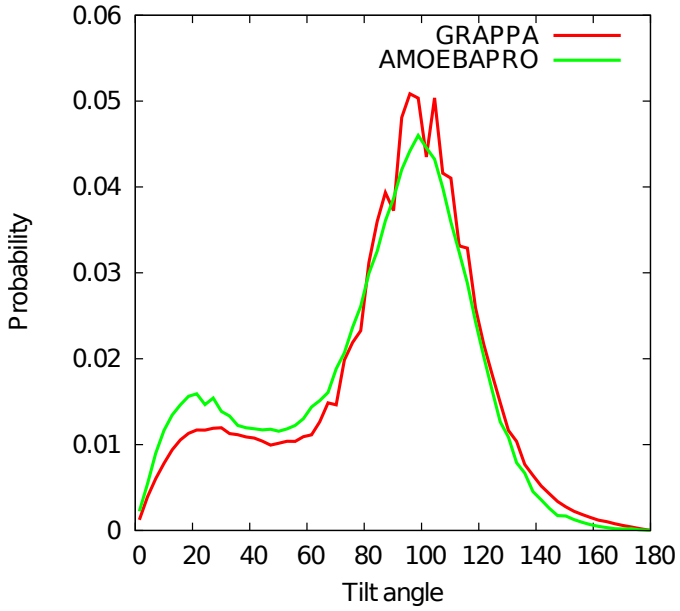

Fig. S6 The probability distribution of the tilt angle between the O-H bond vectors and the normal to the graphene plane for the water molecules in the first solvation layer for both the GRAPPA and AMEOBAPRO FFs.

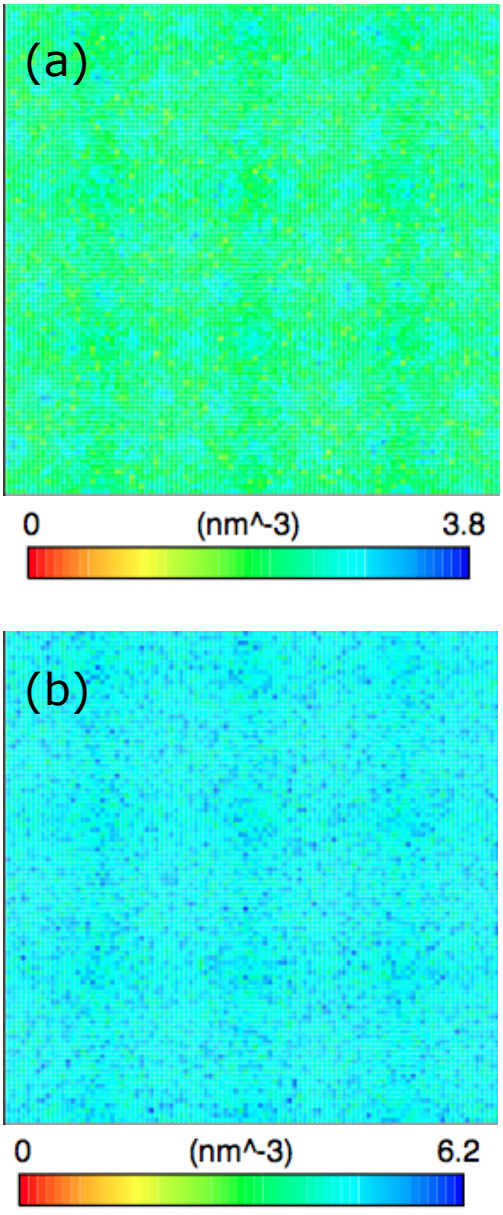

Fig. S7 The 2D number density maps of the (a) oxygen atoms and (b) the hydrogen atoms of water molecules at the graphene-water interface from simulations using the GRAPPA FF.

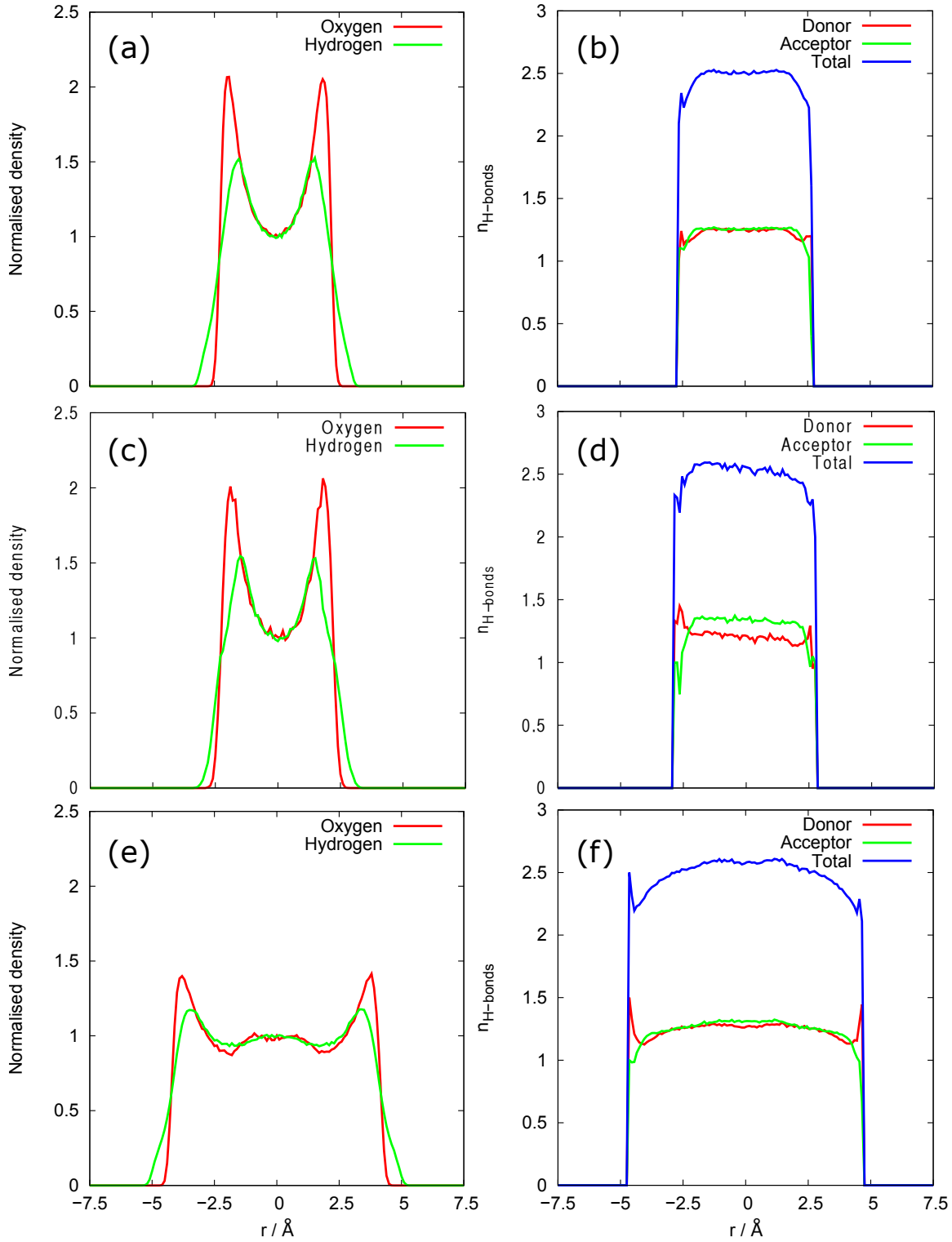

Fig. S8 The density profiles and hydrogen bonding profiles for the simulations of water within carbon nanotubes: (a) density profiles for the (14×0) CNT using GRAPPA, (b) H-bond profiles for the (14×0) CNT using GRAPPA, (c) density profiles for the (14×0) CNT using AMEOBAPRO, (d) H-bond profiles for the (14×0) CNT using AMEOBAPRO (19×0) CNT, (e) density profiles for the (19×0) CNT using GRAPPA and (f) H-bond profiles for the (19×0) CNT using GRAPPA.

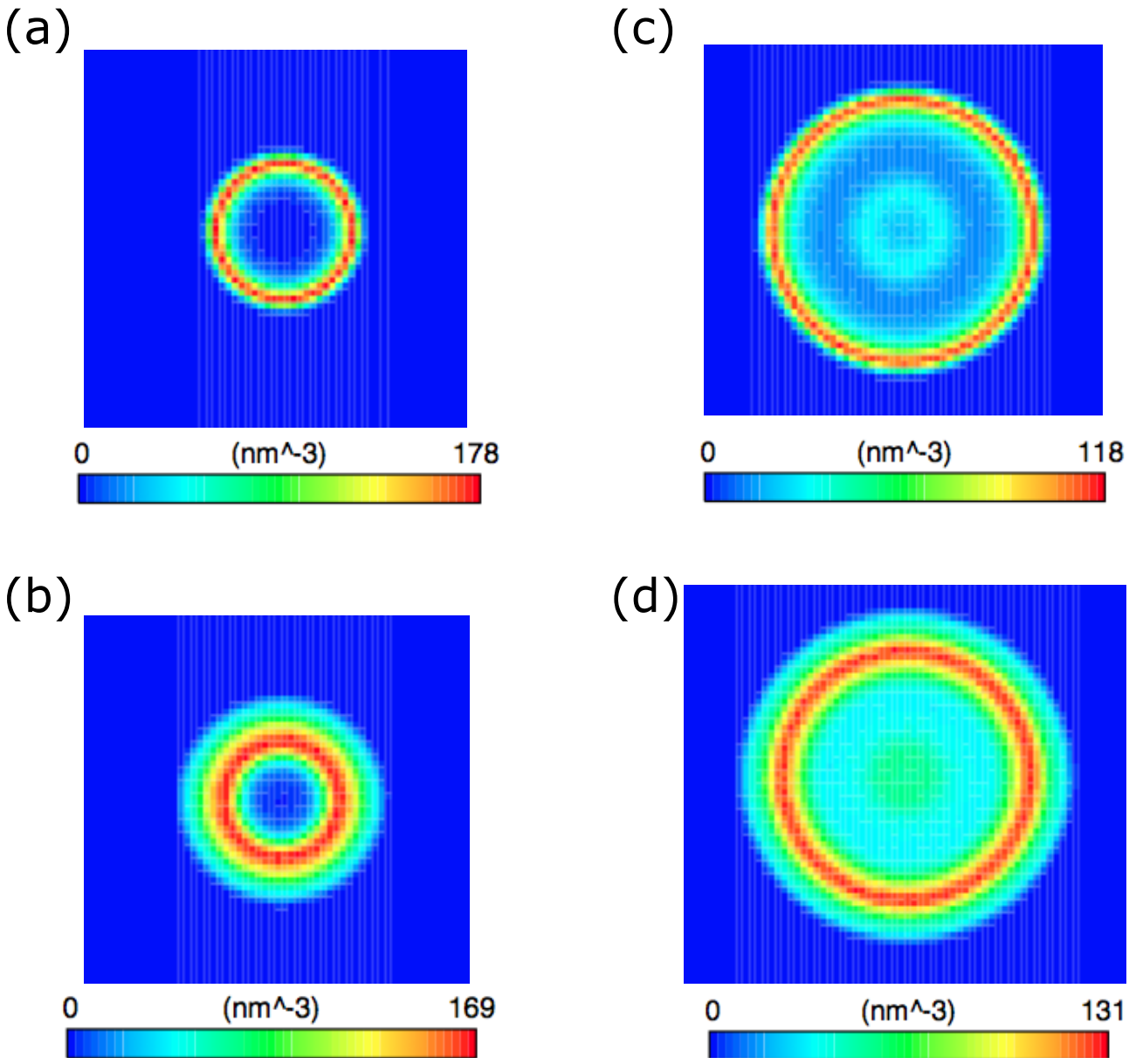

Fig. S9 The 2D number density maps of (a) the water oxygen atoms in the (14×0) CNT, (b) the water hydrogen atoms (14×0) CNT, (c) the water oxygen atoms in the (19×0) and (d) the water hydrogen atoms in the (19×0) CNT from simulations using the GRAPPA FF.

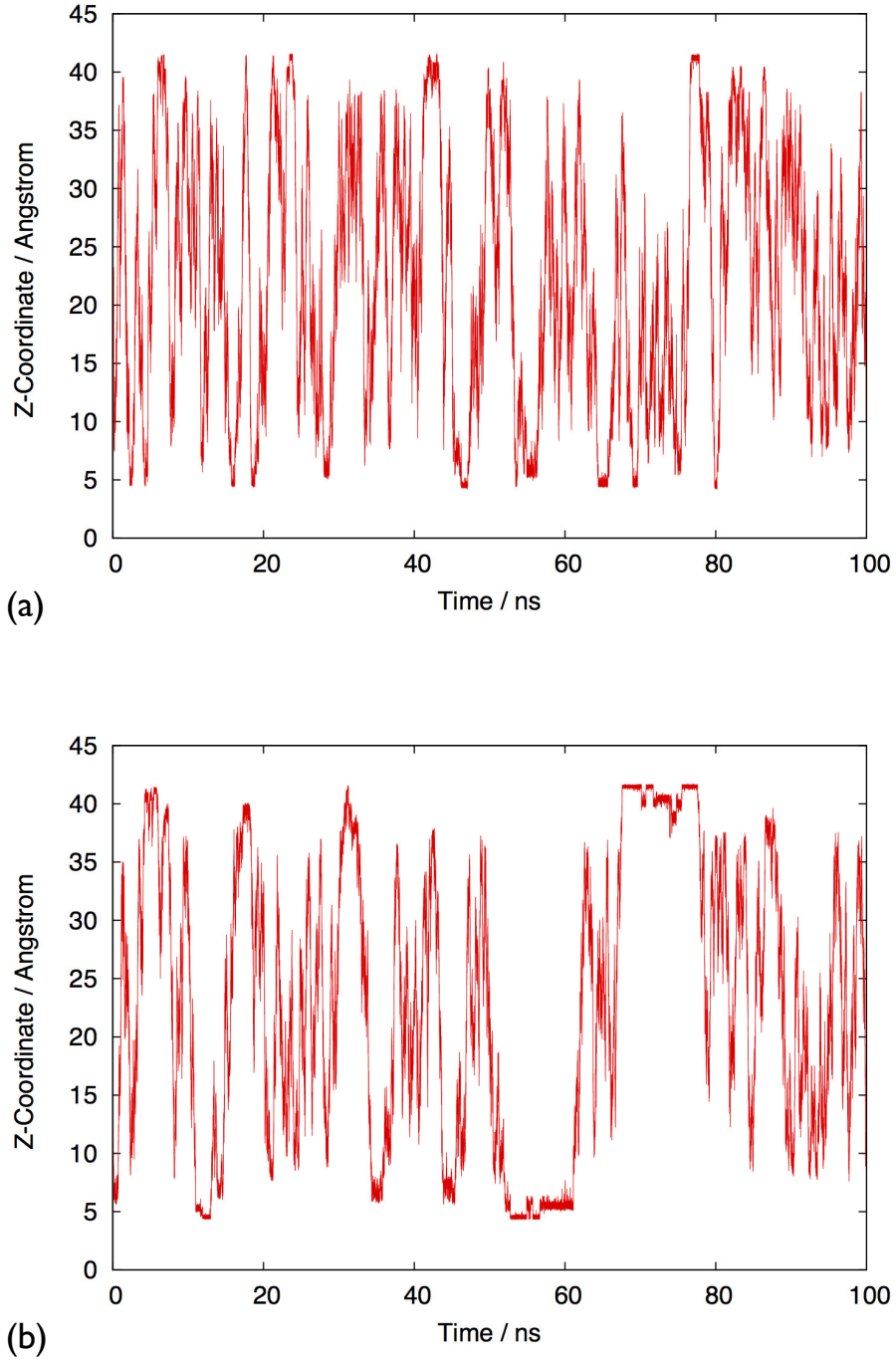

Fig. S10 The collective variable (the centre of mass of the amino acid) as a function of time for the meta-dyanmics simulations of (a) alanine and (b) tryptophan.

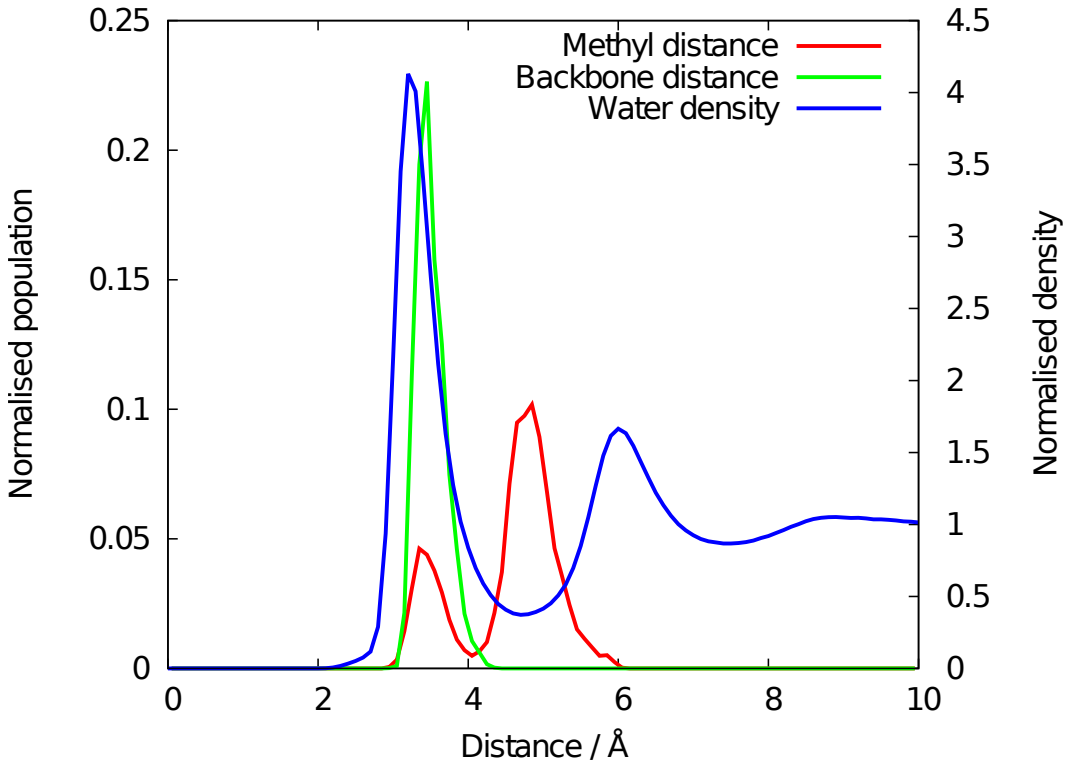

Fig. S11 The probability distribution of the distance between the carbon of the methyl side chain of Ala and the graphene surface, when amide backbone is adsorbed. The density profile of water is also shown for reference.

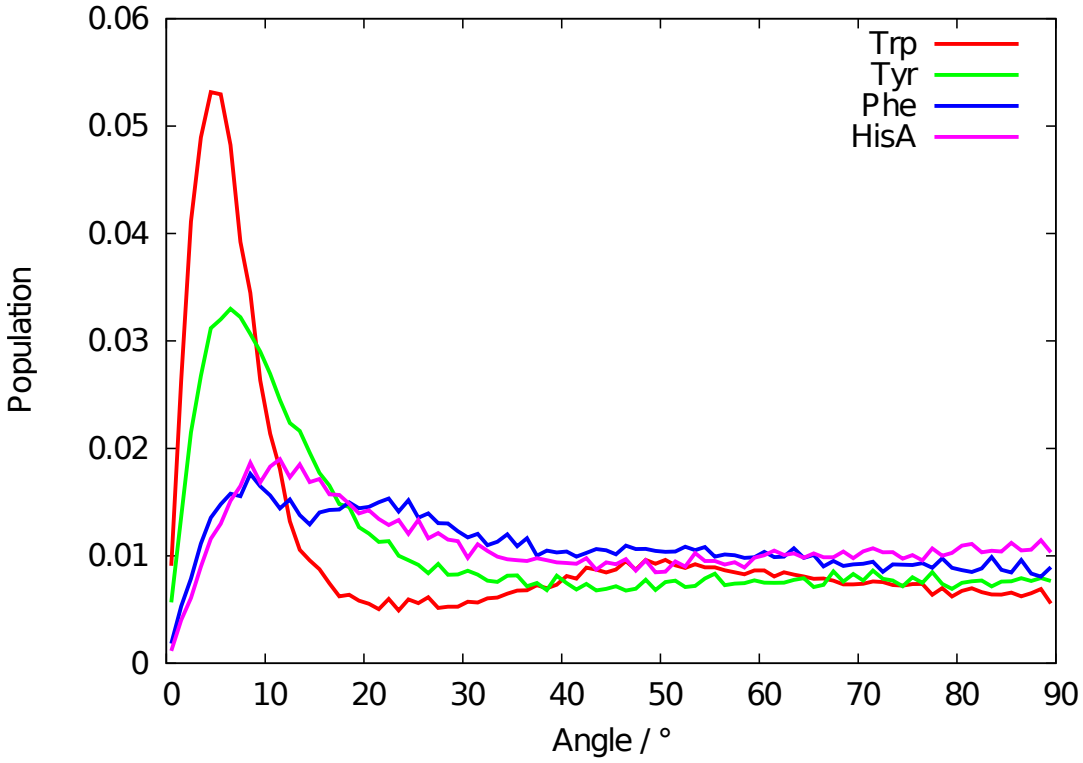

Fig. S12 The probability distribution of the angle between the plane of the aromatic ring and the graphene surface, when the centre of the mass of the amino acid was within 9 Å of the graphene surface, for the aromatic amino acid residues: Trp, Tyr, Phe and HisA.